^{18}F-FDG and ^{18}F-FLT Uptake Early After Cyclophosphamide and mTOR Inhibition in an Experimental Lymphoma Model

Lieselot Brepoels[1,2], Sigrid Stroobants[1,2], Gregor Verhoef[3], Tjibbe De Groot[2,4], Luc Mortelmans[1,2], and Christiane De Wolf-Peeters[5]

[1]Department of Nuclear Medicine, University Hospital Gasthuisberg Leuven, Leuven, Belgium; [2]Molecular Small Animal Imaging Centre, University Hospital Gasthuisberg Leuven, Leuven, Belgium; [3]Department of Hematology, University Hospital Gasthuisberg Leuven, Leuven, Belgium; [4]Laboratory for Radiopharmacy, University Hospital Gasthuisberg Leuven, Leuven, Belgium; and [5]Department of Pathology, University Hospital Gasthuisberg Leuven, Leuven, Belgium

To be a reliable predictor of response, tracer uptake should reflect changes in the amount of active tumor cells. However, uptake of ^{18}F-FDG, the most commonly used PET tracer, is disturbed by the inflammatory cells that appear early after cytotoxic therapy. The first aim of this study was to investigate whether 3′-^{18}F-fluoro-3′-deoxy-L-thymidine (^{18}F-FLT), a marker of cellular proliferation, is a better tracer for response assessment early after cytotoxic therapy. A second objective of this study was to investigate whether ^{18}F-FDG and ^{18}F-FLT responses were comparable early after mammalian target of rapamycin (mTOR) inhibition, as an example of proliferation-targeting therapies. **Methods:** Severe combined immunodeficient mice were subcutaneously inoculated with Granta-519 cells, a human cell line derived from a leukemic mantle cell lymphoma. Half the mice were treated with cyclophosphamide and the other half with mTOR inhibition. ^{18}F-FDG and ^{18}F-FLT uptake was evaluated by small-animal PET on day 0 (D0; before treatment), D+1, D+2, D+4, D+7, D+9, D+11, and D+14. At each time point, 2 mice of each treatment condition were sacrificed, and tumors were excised for histopathology. **Results:** After cyclophosphamide, ^{18}F-FDG and ^{18}F-FLT uptake decreased, with a maximum reduction of −29% for ^{18}F-FDG and −25% for ^{18}F-FLT uptake at D+2, compared with baseline. Although ^{18}F-FDG uptake increased from D+4 on, with a maximum on D+7, ^{18}F-FLT uptake remained virtually stable. Histology showed an increase in apoptotic or necrotic tumor fraction, followed by an influx of inflammatory cells. In mTOR-inhibited mice, ^{18}F-FDG uptake dropped until D+2 after therapy (−43%) but increased at D+4 (−27%) to form a plateau on D+7 and D+9 (−14% and −16%, respectively). Concurrently, ^{18}F-FLT uptake decreased to −31% on D+2, followed by an increase with a peak value of +12% on D+7, after which ^{18}F-FLT uptake decreased again. Cyclin D1 expression dropped from D+1 until D+4 and returned to baseline at D+7. **Conclusion:** Because ^{18}F-FLT uptake is not significantly influenced by the temporary rise in inflammatory cells early after cyclophosphamide, it more accurately reflects tumor response. However, a formerly unknown temporary rise in ^{18}F-FLT uptake

a few days after the administration of mTOR inhibition was defined, which makes it clear that drug-specific responses have to be considered when using PET for early treatment monitoring.

Key Words: therapy response; ^{18}F-FLT; ^{18}F-FDG; PET; lymphoma

Uptake of ^{18}F-FDG is closely related to the metabolic activity and the number of viable tumor cells; because a reduction in metabolism and proliferation of the damaged cells and a reduced number of viable cells occur within a few days after chemotherapy, effective therapy results in a subsequent reduction of the ^{18}F-FDG uptake measured using PET.

Römer et al. were the first to document a rapid decrease of ^{18}F-FDG uptake in non-Hodgkin lymphoma (NHL) as early as 7 d after treatment (*1*). However, a significant number of patients still have residual ^{18}F-FDG uptake 1 wk after treatment, and it was hypothesized that assessment of response early after therapy requires quantification of ^{18}F-FDG uptake and the use of cutoff values. Until now, no threshold was defined that allowed the prediction of relapse in the first days after therapy in lymphoma (*2*). It is possible that quantification of response assessment at this time is too variable because of interfering factors such as inflammation. Shortly after the administration of cytotoxic therapy (e.g., cyclophosphamide)—which acts through the cross-linking of DNA and the induction of apoptosis or necrosis—an influx of activated inflammatory cells occurs, making it difficult to correctly quantify tumor response. In previous work, we showed that this influx can be suppressed by the administration of corticosteroids (*3,4*).

Alternatively, other tracers (e.g., 3′-^{18}F-fluoro-3′-deoxy-L-thymidine [^{18}F-FLT]) can be used for treatment monitoring. ^{18}F-FLT is monophosphorylated by cytosolic thymidine

kinase-1 (TK1), which leads to intracellular trapping. Because TK1 increases just before and in the S phase, ^{18}F-FLT uptake is cell cycle–dependent and is assumed to reflect the amount of active proliferating cells (5). Because inflammatory cells have only a minor tendency to proliferate once they enter the tumor, the ^{18}F-FLT uptake, compared with ^{18}F-FDG uptake, in tumor lesions is less hampered by this inflammatory response; ^{18}F-FLT uptake may reflect more accurately the obtained treatment response. However, ^{18}F-FLT is only insignificantly incorporated into DNA and TK1 may be upregulated, despite an inhibition of the DNA synthesis. The first aim of this study was to investigate in vivo whether ^{18}F-FLT is a better tracer for response assessment in the first days after cytotoxic therapy.

Most recent advances in cancer treatment have come from the development of disease-specific molecule-targeted agents, instead of from the empiric combinations of cytotoxic agents from the past. Many of these drugs induce cell cycle arrest instead of tumor cell death and are not expected to induce fast tumor regression, making measurements of cellular viability by ^{18}F-FDG theoretically less relevant. The assessment of cellular proliferation by ^{18}F-FLT might be an alternative. An example of these new strategies is the inhibition of the mammalian target of rapamycin (mTOR). mTOR is a regulator of cellular proliferation and acts through several targets. One of these targets is the messenger RNA (mRNA) encoding for the cyclin D1 protein, which makes this strategy extremely interesting for the treatment of mantle cell lymphoma (MCL) (6). This subtype of B-cell NHL is characterized by translocation t(11;14) connecting the cyclin D1 gene with the promoter region of the immunoglobulin heavy chain. As a result, the cyclin D1 gene is constitutively transcribed to cyclin D1 mRNA, which leads to an overexpression of the cyclin D1 protein. Cyclin D1, at its turn, induces the progression of the cell cycle through the G_1–S phase. The blocking of mTOR leads to an inhibition of the translation of cyclin D1 mRNA to the cyclin D1 protein and provokes cell cycle arrest in mid to late G1.

Especially after the administration of proliferation-targeting therapies, the time course of ^{18}F-FDG and ^{18}F-FLT uptake has not yet been properly explored. Therefore, a second objective of this study was to investigate whether ^{18}F-FDG and ^{18}F-FLT responses were comparable early after mTOR inhibition.

MATERIALS AND METHODS

Animal Model

Six-week-old male severe combined immunodeficient (SCID) mice (C.B-17/Icr SCID/SCID) were inoculated with 5.10^6 Granta-519 cells, subcutaneously in the left shoulder and the right thigh. The Granta-519 cell line was obtained from the DMSZ tissue bank. This cell line is derived from a leukemic MCL and carries t(11;14) associated with cyclin D1 overexpression. Treatment with cyclophosphamide or temsirolimus was started when the tumor reached a diameter of 10–15 mm.

Experimental Design

A total of 46 mice were used for analysis. Two mice were sacrificed when their tumor diameter reached 15 mm; these mice did not receive any treatment. Their tumors were dissected for histopathology and used as baseline references.

The other mice were divided into 2 treatment regimens. The first group ($n = 22$) was treated with a single dose of cyclophosphamide (125 mg/kg intraperitoneally) (Endoxan; Baxter) on day 0 (D0). The second group ($n = 22$) received temsirolimus (50 mg/kg intraperitoneally), which was provided by Wyeth (CCI-779, Torisol). Temsirolimus is one of the first mTOR inhibitors currently tested in clinical studies for the treatment of patients with relapsed MCL (7). ^{18}F-FDG and ^{18}F-FLT uptake over time was evaluated by serial small-animal PET (5 mice per treatment per tracer) on D0 (before treatment), D+1, D+2, D+4, D+7, D+9, D+11, and D+14. At each time, 2 mice of each treatment condition were sacrificed, and tumors were excised for histopathology (Table 1).

Small-Animal PET

After overnight fasting, the mice underwent small-animal PET (Focus 220 microPET; Concorde-CTI/Siemens). Spatial resolution of the used PET system is 1.6 mm, and acquired images were reconstructed with ordered-subsets expectation maximization.

TABLE 1. Flow Chart of Experimental Design

Treatment	Tracer	D0*	D+1	D+2	D+4	D+7	D+9	D+11	D+14
Cyclophosphamide ($n^†$ = 22)		x‡							
Small-animal PET	^{18}F-FDG	$n = 5$	x	x	x	x	x	x	x + histology
	^{18}F-FLT	$n = 5$	x	x	x	x	x	x	x + histology
Histology			$n = 2$	$n = 2$	$n = 2$	$n = 2$	$n = 2$	$n = 2$	
Temsirolimus ($n = 22$)		x							
Small-animal PET	^{18}F-FDG	$n = 5$	x	x	x	x	x	x	x + histology
	^{18}F-FLT	$n = 5$	x	x	x	x	x	x	x + histology
Histology			$n = 2$	$n = 2$	$n = 2$	$n = 2$	$n = 2$	$n = 2$	
Reference mice ($n = 2$)									
Histology		$n = 2$							

*D0 is before treatment, D + x is on day x after treatment.
†Number of mice used.
‡This was done on this specific day.

Simulations with spheres of different diameters with these settings showed that effects of partial volume on ^{18}F-FDG uptake were minimal in lesions with a diameter larger than 3 mm.

After the mice were sedated by gas anesthesia (isoflurane, Forene; Abbot), tumor dimensions were measured (caliper) and body weight and glycemia were determined. Sixty minutes after an injection of ^{18}F-FDG (8–11 MBq) via a tail vein, small-animal PET was performed (10 min) at a single-bed position with the tumor in the center of the field. All animals received an intramuscular injection of furosemide (40 mg/kg) (Lasix; Aventis) in the contralateral thigh at the same time as the tracer injection, to reduce reconstruction artifacts caused by the high concentration of ^{18}F-FDG in the urine; the bladder was carefully voided before scanning.

^{18}F-FDG and ^{18}F-FLT PET Evaluation

The same methodology as described in previous work was used to quantify ^{18}F-FDG and ^{18}F-FLT uptake in the tumor lesion (4). Because of the frequent occurrence of central necrosis and low tumor-to-background ratios for ^{18}F-FLT, this analysis was based on maximal standardized uptake values (SUVs).

Change in SUV was expressed as a percentage of the baseline SUV on D0. To correct for differences in administered dose (paravenous injections became more frequent after several injections in the same mouse), all SUVs were normalized by dividing maximal SUVs of the tumor by the corresponding mean SUV in a standard region in the liver as a reference value. This standard region was defined as a circular region of interest of about 0.8 mm diameter in a homogeneous part of the liver. All further reported SUVs are maximal SUVs normalized for liver uptake.

Histology

Paraffin-embedded sections were stained with hematoxylin and eosin. Immunohistochemical staining was performed with antiCD20 mAb (pan B-cell marker), with Mib-1, cyclin D1, and proliferating cell nuclear antigen (PCNA). Although Mib-1 recognizes an epitope of the Ki67 nuclear antigen that is present during DNA synthesis (all cells currently in the cell cycle, not in G0), PCNA protein expression is associated with late G1 or S phase in normal cells (S phase).

Every fifth microscopic field of viable-looking tumor tissue was semiquantitatively scored for the number of CD20-, Mib-1–, PCNA-, and cyclin D1–positive cells of the total number of viable tumor cells, and a mean value was estimated ($-$ [<25%, almost none]; $+$ [some, 25%–50%]; $++$ [a lot, 50%–75%]; and $+++$ [almost all, 75%–100%]).

Statistics

For each time point, the mean $\pm$ SEM in both treatment groups was calculated and expressed graphically. A 2-tailed P value of less than or equal to 0.05 was considered statistically significant. Unpaired Student t tests were used to evaluate differences between the 2 treatment groups, and paired Student t tests were performed for differences between time points on the activity curve within 1 treatment condition.

RESULTS

Baseline ^{18}F-FLT and ^{18}F-FDG Uptake

All tumors had visible ^{18}F-FLT and ^{18}F-FDG uptake, and almost all tumors had a central zone of low tracer uptake. Mean SUV_{FDG} at baseline was 3.1 (range, 2.4–4.8), and mean SUV_{FLT} at baseline was 2.1 (range, 1.7–2.4). Baseline ^{18}F-FDG uptake was significantly higher than ^{18}F-FLT uptake ($P < 1.10^{-7}$).

Decrease in ^{18}F-FLT and ^{18}F-FDG Uptake in Cyclophosphamide-Treated Mice

Figure 1 shows an example of the evolution of ^{18}F-FDG and ^{18}F-FLT uptake after the administration of cyclophosphamide. ^{18}F-FDG and ^{18}F-FLT uptake decreased shortly after the administration of cyclophosphamide, with a maximum reduction of -29% for ^{18}F-FDG and -25% for ^{18}F-FLT uptake at D+2, compared with baseline values
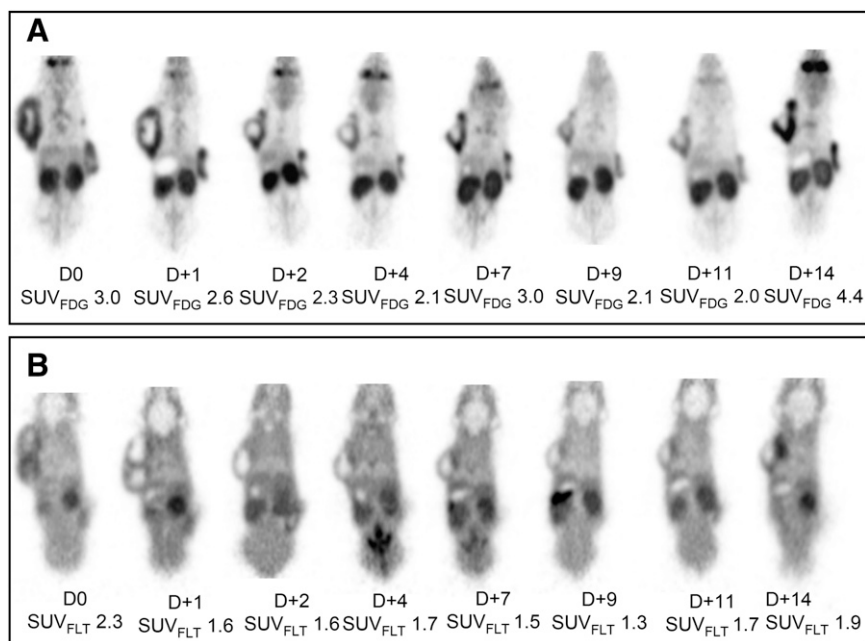

FIGURE 1. Example of serial small-animal PET images on D0 and on D+1, D+2, D+4, D+7, D+9, D+11, and D+14 after treatment with cyclophosphamide as measured with ^{18}F-FDG (A) and ^{18}F-FLT (B) PET.
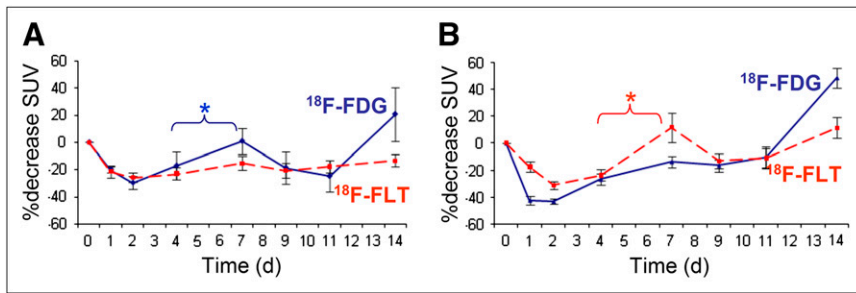
FIGURE 2. ^{18}F-FDG and ^{18}F-FLT uptake as measured by serial small-animal PET and expressed as mean SUV$_{FDG}$ and mean SUV$_{FLT}$ ± SEM in mice treated with cyclophosphamide (A), compared with mice treated with temsirolimus (B). Blue curve = percentage decrease in SUV$_{FDG}$; red curve = SUV$_{FLT}$. *Significant at the $P \leq 0.05$ level.

(Fig. 2A). Although ^{18}F-FDG uptake increased from D+4 on, with a maximum on D+7 (+1% increase, compared with baseline), ^{18}F-FLT uptake remained virtually stable (−16% at D+7, compared with baseline). After this temporary increase, ^{18}F-FDG uptake decreased again at D+9 (−19%) and D+11 (−25%) and increased again at D+14 (+20%).

The difference in ^{18}F-FDG uptake between D+4 and D+7 was highly significant ($P = 0.0005$). No significant difference could be retained for ^{18}F-FLT uptake between D+4 and D+7 ($P = 0.48$) (Table 2). No significant difference between the slopes of ^{18}F-FLT uptake and ^{18}F-FDG uptake was observed ($P = 0.13$).

Decrease in ^{18}F-FLT and ^{18}F-FDG Uptake in Temsirolimus-Treated Mice

In temsirolimus-treated mice, ^{18}F-FDG uptake dropped at D+1 and D+2 after therapy (−43% on D+2, compared with baseline) but increased at D+4 (−27%, compared with baseline) to form a plateau on D+7 and D+9 (−14% and −16%), after which ^{18}F-FDG uptake increased on D+14 (Figs. 2B and 3).

Concurrently, ^{18}F-FLT uptake decreased after temsirolimus administration, until a maximum decrease of −31% on D+2, and then importantly increased with a peak value of +12%, compared with baseline, on D+7. After this temporary increase, ^{18}F-FLT uptake decreased (−13% and −11% on D+9 and D+11, respectively), only to increase on D+14 (+11%).

Histopathology in Untreated Mice

In untreated animals, tumors were composed of a massive proliferation of CD20-positive cells with positivity for Mib-1 and PCNA, with high cyclin D1 expression and the presence of multiple mitotic figures. Baseline tumors had a significant necrotic fraction, even before any treatment was started, and some nontumor, inflammatory cells were present, mainly macrophages.

Histopathology in Cyclophosphamide-Treated Mice

After the administration of cyclophosphamide, there was an increase in apoptotic or necrotic tumor fraction from D+4 to D+9. This rise in apoptotic or necrotic cells is followed by an increasing number of inflammatory cells, with a maximum on D+9 to make place for fibrosis a few days later at D+14.

The number of cyclin D1–positive cells decreased on D+1 and D+2, with a slow increase in the number of cyclin D1–positive cells from D+4 until baseline values were reached on D+9. No clear responses were seen in the number of Mib-1– and PCNA-positive cells (Table 3; Fig. 4).

Histopathology in Temsirolimus-Treated Mice

Temsirolimus induced an increase in the apoptotic or necrotic cell fraction at D+2 after therapy. Compared with cyclophosphamide-treated mice, a more pronounced inflammatory reaction was observed at D+2 to D+4, which consisted largely of macrophages but also of some granulocytes.

Cyclin D1 expression dropped from D+1 until D+4 and returned to baseline at D+7. Concurrently with the decrease in cyclin D1, Mib-1 expression decreased, although the decrease was less pronounced. At D+9 after therapy, morphology of the tumor had returned to baseline appearance, with a high cyclin D1 and Mib-1 expression. Tumor volume increased spectacularly at D+14, because of tumor regrowth. No changes were observed in PCNA expression (Table 4; Fig. 4).

DISCUSSION

Because patients with poor prognosis may benefit from early intensified treatment regimens, it is useful to know the individual patient's risk of relapse as early as possible. The rationale for performing PET early during therapy lies in the detection of resistant tumor clones that respond to treatment more slowly than chemosensitive tumor cells and

TABLE 2. Comparison of SUV$_{FDG}$ and SUV$_{FLT}$ at Days 4 and 7

Treatment	Tracer SUV	D+4 (%)	D+7 (%)	P
Cyclophosphamide	^{18}F-FDG	−25.09	−3.91	0.00005*
	^{18}F-FLT	−26.07	−18.82	0.48
Temsirolimus	^{18}F-FDG	−26.58	−12.58	0.09
	^{18}F-FLT	−21.09	−21.09	0.004*

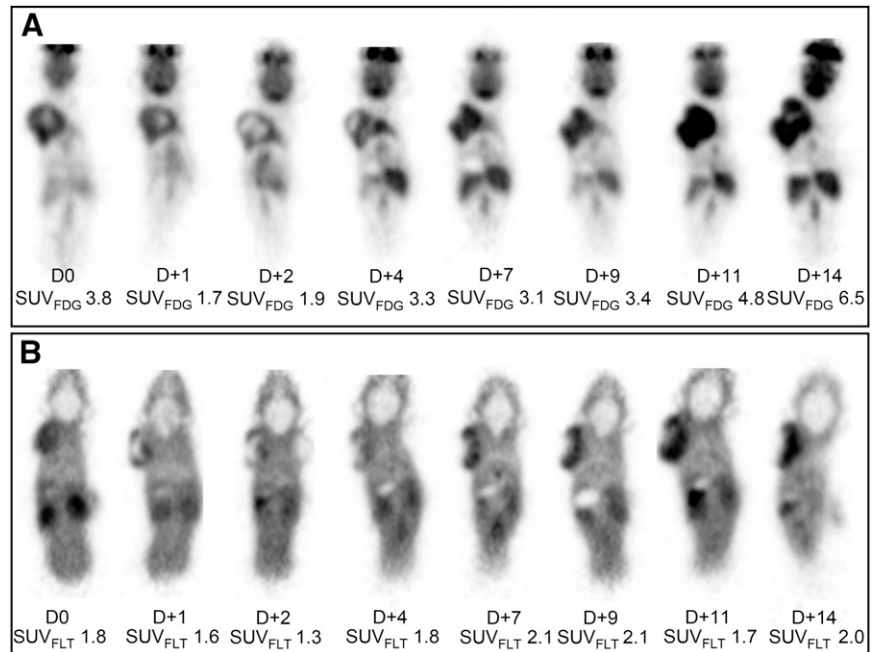*Statistically significant at the $P \leq 0.05$ level.

FIGURE 3. Example of serial small-animal PET images on D0 and on D+1, D+2, D+4, D+7, D+9, D+11, and D+14 after treatment with temsirolimus and measured with ^{18}F-FDG (A) and ^{18}F-FLT (B) PET.

may eventually cause disease relapse or progression. However, early after therapy, an inflammatory reaction occurs that mainly consists of macrophages for the removal of necrotic debris. Because these inflammatory cells also show high ^{18}F-FDG uptake, their presence will disturb measurements of the tumor response. This study evaluated whether ^{18}F-FLT was a more reliable tracer for quantification of response, because ^{18}F-FLT is more tumor-specific than ^{18}F-FDG and is believed to reflect the amount of active proliferating cells. Concurrently, ^{18}F-FDG and ^{18}F-FLT responses were compared after the administration of temsirolimus (a cell cycle–targeting agent).

A significantly lower baseline ^{18}F-FLT uptake than ^{18}F-FDG uptake was found, which has already been reported for several other tumor types (8–12) and which made it difficult to adequately delineate tumor volume in ^{18}F-FLT images. Therefore, this analysis concentrated on the maximal SUVs, the most frequently used parameter for response

assessment because of the relative resistance of maximal SUVs to partial-volume effects and interobserver variability.

Our results in cyclophosphamide-treated mice showed a significant increase in ^{18}F-FDG uptake from D+4 to D+7, which was not present for ^{18}F-FLT uptake. This finding confirms the hypothesis that the temporary rise in inflammatory cells does not significantly influence ^{18}F-FLT uptake. Therefore, ^{18}F-FLT uptake after therapy is less disturbed by this reaction and is more reflective of tumor tissue than is ^{18}F-FDG uptake after the administration of cyclophosphamide. This finding corresponds to the many reports on the low uptake of ^{18}F-FLT in inflammatory lesions (13,14). However, the initial enthusiasm about the higher specificity of ^{18}F-FLT has been tempered by the recent reports that ^{18}F-FLT uptake also occurs in granulomatous inflammatory lesions such as tuberculosis (15) and in reactive lymph nodes (16,17) (related to a high proliferation rate of macrophages and B-lymphocytes, respectively).

TABLE 3. Semiquantitative Scoring of Number of Considered Cells on Total Number of Viable Cells in Cyclophosphamide-Treated Mice

Day	Tumor cells	Apoptosis/necrosis	Inflammatory mouse cells	Mib-1	Cycline D1
0*	+++	+	+	++/+++	+++
+1	+++	+	+	++	++
+2	++	++	−/+	++/+++	++
+4	++	+/++	+	++/+++	++
+7	++	+/++	+	++/+++	+/++
+9	++	++	++	+/++	++/+++
+11	+++	+	+	++/+++	+++
+14	++/+++	++	−/+	++/+++	+++

*D0 is before treatment, D + x is on day x after treatment.
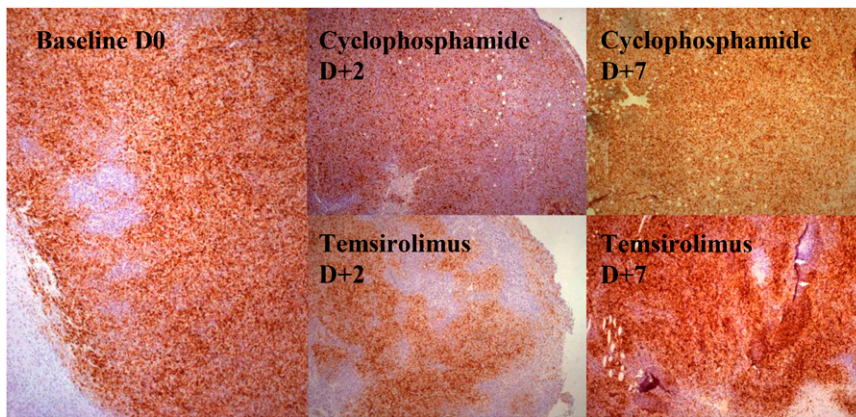− = almost none; + = some; ++ = a lot; +++ = almost all.

FIGURE 4. Immunohistochemical staining for cyclin D1 at day 0 (before) and at D+2 and D+7 after treatment. Staining for cyclin D1 shows moderate decrease in cyclin D1–positive tumor cells after 2 d of treatment with cyclophosphamide. After administration of temsirolimus, important decrease in amount of cyclin D1–positive tumor cells was seen at D+2, which increased again on day 7.

After the administration of temsirolimus, ^{18}F-FDG uptake dropped spectacularly at D+1 and D+2 but increased at D+4, after which ^{18}F-FDG uptake remained almost steady for another 7 d. This result corresponds to the histologic finding that in temsirolimus-treated mice, tumor response occurs earlier and more dramatically than in cyclophosphamide-treated mice. The inflammatory reaction in these mice is also present earlier than in cyclophosphamide-treated mice, which may explain why ^{18}F-FDG uptake increased at D+4. The subsequent plateau from D+7 to D+11 is probably a summation of a decline in inflammatory ^{18}F-FDG uptake and a reactivation of the tumor cells.

Concurrently with the decrease in ^{18}F-FDG uptake, ^{18}F-FLT decreased at D+1 and D+2 after the administration of temsirolimus. At D+4, ^{18}F-FLT uptake after temsirolimus administration increased to form a significant peak at D+7, after which ^{18}F-FLT uptake dropped again on D+9. Until now, no comparable finding has been described, and the exact mechanism of this finding remains unclear.

The increase in ^{18}F-FLT uptake on D+7 cannot be attributed to an inflammatory reaction because of the absence of matching histopathologic findings; thus, the explanation lies in ^{18}F-FLT uptake by the tumor cells themselves. The increased expression of cyclin D1 at this time suggests that the tumor cells have regained their translation capacity of cyclin D1 and consequently their proliferation capacity (half-life of temsirolimus, 9–17 h) (Wyeth investigational brochure, April 2008). This explanation is consistent with previous reports that the still-viable tumor cells reenter into S phase within 2–4 h after removal of the drug, which leads to an elevated TK1 (5,18–20). However, an increase in ^{18}F-FLT uptake can also be a result of activated cellular repair mechanisms, a stimulation of the salvage pathway of the pyrimidine metabolism, or the antiangiogenic effect of temsirolimus that was shown in breast cancer and may have led to alterations in tracer availability at the tumor site (18). Therefore, in future work, it is important to correlate our findings with an evaluation of TK1 activity and DNA flow cytometry to obtain a more sustained insight on the provoking mechanism of this finding.

^{18}F-FLT uptake was shown to be largely drug-dependent in cell lines, with a 7- to 10-fold increase in ^{18}F-FLT uptake after treatment with 5-fluorouracil (5-FU), attributed to a blocking of the de novo pathway of the pyrimidine metabolism with a redistribution of nucleoside transporters to the plasma membrane and an accumulation of 5-FU–treated cells in early S phase (21). In contrast, ^{18}F-FLT uptake after cisplatin administration was reduced, despite considerable S-phase arrest (22).

In targeted therapies, Solit et al. showed that mitogen-activated protein kinase/extracellular signal-regulated ki-

TABLE 4. Semiquantitative Scoring of Number of Considered Cells on Total Number of Viable Cells in Temsirolimus-Treated Mice

Day	Tumor cells	Apoptosis/necrosis	Inflammatory mouse cells	Mib-1	Cycline D1
0*	+++	+	+	++/+++	+++
+1	++/+++	++	+	+/++	+/++
+2	++	+++	+/++	++	+
+4	++	++/+++	+/++	++	+
+7	++	+	++	+++	++/+++
+9	++	+	+	++	++
+11	+	−	+	+++	++/+++
+14	++/+++	+	+	+++	+/++

*D0 is before treatment, D + x is on day x after treatment.
− = almost none; + = some; ++ = a lot; +++ = almost all.

nase (MEK), which causes G1 arrest and downregulation of cyclin D1 expression, leads to a significant decrease in ^{18}F-FLT uptake 1 wk after treatment (*23*). In a mouse follicular lymphoma xenotransplant model, a significant decrease of ^{18}F-FLT uptake was observed at 48 h after chemotherapy with cyclophosphamide (*24*). Comparable results were obtained with preclinical models of sarcoma after cisplatin administration (*8*), esophageal carcinoma after chemoradiation (*25*), and squamous cell carcinoma 24 h after irradiation (*26*).

Recently, Herrman et al. evaluated ^{18}F-FLT PET for early response monitoring in 22 patients with high-grade NHL and showed that ^{18}F-FLT uptake in lymphoma is decreased 2 d after treatment with cyclophosphamide, doxorubicin, vincristine, and prednisone but not after rituximab (*27*).

Until now, no authors, to our knowledge, have monitored the time course of ^{18}F-FLT uptake at several time points during the first days after treatment, although by comparing baseline ^{18}F-FLT uptake with a single time point after treatment, information about time-dependent processes can be masked, certainly interfering with PET results. The flipside of monitoring multiple time points in the same animals is the absence of histologic or cytologic data of the scanned animal itself and a more hampered correlation of PET results with ex vivo tumor evaluation.

The main limitation of this study is without a doubt the mouse model. The tumor model involves an immune-deficient animal (SCID mice) without a functional T or B cell compartment, and extrapolation of our results to immune-competent mice or humans is, therefore, not possible. Despite these limitations, SCID mice have a normal macrophage, granulocyte, and natural killer function, and an inflammatory reaction was shown in this tumor model at about D+7 in earlier experiments (*4,28*).

Each of the used treatment strategies has inevitable influences on the immune system. Cyclophosphamide is used for immune suppression, and temsirolimus is a potent inhibitor of lymphocyte proliferation and cytokine production and is currently being tested for the treatment of rheumatoid arthritis. Although temsirolimus will probably have only minor influences on our tumor model (no functional T and B cells in SCID mice), these are likely to interfere with the normal clinical situation. Another drawback of this study is that it does not include dynamic scans, which could have allowed a more thorough insight into the dynamics of tracer uptake as a response to therapy.

The objective of this study was to investigate how ^{18}F-FDG and ^{18}F-FLT uptake changed in the first days after therapy and whether different treatment strategies require other interpretations of uptake quantification. It was not our objective to compare action mechanisms of the different drugs or to compare the efficacy of treatments with each other; consequently, this investigation does not allow conclusions about the drugs used, only about their effect on tracer uptake early after therapy.

CONCLUSION

This investigation showed that the used treatment strategy influences ^{18}F-FDG and ^{18}F-FLT uptake in different ways, with different time–activity curves shortly after therapy. The temporary rise in ^{18}F-FDG uptake at day 7 after cyclophosphamide administration, attributable to a temporary influx of inflammatory cells, did not alter ^{18}F-FLT measurements. Therefore, ^{18}F-FLT uptake is a more accurate measurement for tumor response than is ^{18}F-FDG uptake after the administration of cyclophosphamide.

However, a formerly unknown temporary rise in ^{18}F-FLT uptake occurred a few days after the administration of temsirolimus had been defined and was related to an increased expression of cyclin D1. The increased expression of cyclin D1 probably points to a reactivation of the tumor cells; however, the exact underlying mechanism of the temporary rise in ^{18}F-FLT uptake remains to be established on the molecular level.

Our results make it clear that not only with ^{18}F-FDG PET, but even more with ^{18}F-FLT PET, is the timing of response assessment crucial because of temporary metabolic changes.

REFERENCES

1. Römer W, Hanauske AR, Ziegler S, et al. Positron emission tomography in non-Hodgkin's lymphoma: assessment of chemotherapy with fluorodeoxyglucose. *Blood.* 1998;91:4464–4471.
2. Brepoels L, Stroobants S, De Wolf-Peeters C, Verhoef G. Prospective evaluation on the value of FDG-PET/CT for response assessment in DLBCL after 1 week of R-CHOP [abstract]. *Ann Oncol.* 2008;19(suppl 4):204P.
3. Kubota R, Yamada S, Kubota K, Ishiwata K, Tamahashi N, Ido T. Intratumoral distribution of fluorine-18-fluorodeoxyglucose in vivo: high accumulation in macrophages and granulation tissues studied by microautoradiography. *J Nucl Med.* 1992;33:1972–1980.
4. Brepoels L, Stroobants S, Vandenberghe P, et al. Effect of corticosteroids on ^{18}F-FDG uptake in tumor lesions after chemotherapy. *J Nucl Med.* 2007;48:390–399.
5. Mier W, Haberkorn U, Eisenhut M. [^{18}F]FLT: portrait of a proliferation marker. *Eur J Nucl Med Mol Imaging.* 2002;29:165–169.
6. Hay N, Sonenberg N. Upstream and downstream of mTOR. *Genes Dev.* 2004;18:1926–1945.
7. Costa LJ. Aspects of mTOR biology and the use of mTOR inhibitors in non-Hodgkin's lymphoma. *Cancer Treat Rev.* 2007;33:78–84.
8. Leyton J, Latigo JR, Perumal M, Dhaliwal H, He Q, Aboagye EO. Early detection of tumor response to chemotherapy by 3′-deoxy-3′-[^{18}F]fluorothymidine positron emission tomography: the effect of cisplatin on a fibrosarcoma tumor model in vivo. *Cancer Res.* 2005;65:4202–4210.
9. Cobben DC, van der Laan BF, Maas B, et al. ^{18}F-FLT PET for visualization of laryngeal cancer: comparison with ^{18}F-FDG PET. *J Nucl Med.* 2004;45:226–231.
10. Smyczek-Gargya B, Fersis N, Dittmann H, et al. PET with [^{18}F]fluorothymidine for imaging of primary breast cancer: a pilot study. *Eur J Nucl Med Mol Imaging.* 2004;31:720–724.
11. Francis DL, Visvikis D, Costa DC, et al. Assessment of recurrent colorectal cancer following 5-fluorouracil chemotherapy using both ^{18}FDG and ^{18}FLT PET. *Eur J Nucl Med Mol Imaging.* 2004;31:928.
12. Buck AK, Halter G, Schirrmeister H, et al. Imaging proliferation in lung tumors with PET: ^{18}F-FLT versus ^{18}F-FDG. *J Nucl Med.* 2003;44:1426–1431.

13. Buck AK, Bommer M, Stilgenbauer S. Molecular imaging of proliferation in malignant lymphoma. *Cancer Res.* 2006;66:11055–11061.

14. Been LB, Suurmeijer AJ, Cobben DC, Jager PL, Hoekstra HJ, Elsinga PH. [18F]FLT-PET in oncology: current status and opportunities. *Eur J Nucl Med Mol Imaging.* 2004;31:1659–1672.

15. Zhao S, Kuge Y, Nakada K, et al. 11C-Methionine but not 18F-FDG and 18F-FLT can differentiate tumor from granuloma in experimental rat models [abstract]. *J Nucl Med.* 2006;47(suppl 1):177P.

16. Troost EG, Vogel WV, Merkx MA, et al. 18F-FLT PET does not discriminate between reactive and metastatic lymph nodes in primary head and neck cancer patients. *J Nucl Med.* 2007;48:726–735.

17. Buck AK, Hetzel M, Schirrmeister H, et al. Clinical relevance of imaging proliferative activity in lung nodules. *Eur J Nucl Med Mol Imaging.* 2005;32:525–533.

18. Del Bufalo D, Ciuffreda L, Trisciuoglio D, et al. Antiangiogenic potential of the mammalian target of rapamycin inhibitor temsirolimus. *Cancer Res.* 2006;66:5549–5554.

19. Dumont FJ, Su Q. Mechanism of action of the immunosuppressant rapamycin. *Life Sci.* 1996;58:373–395.

20. Haberkorn U, Altmann A, Kamencic H, et al. Glucose transport and apoptosis after gene therapy with HSV thymidine kinase. *Eur J Nucl Med.* 2001;28:1690–1696.

21. Perumal M, Pillai RG, Barthel H, et al. Redistribution of nucleoside transporters to the cell membrane provides a novel approach for imaging thymidylate synthase inhibition by positron emission tomography. *Cancer Res.* 2006;66:8558–8564.

22. Dittmann H, Dohmen BM, Kehlbach R, et al. Early changes in [18F]FLT uptake after chemotherapy: an experimental study. *Eur J Nucl Med Mol Imaging.* 2002;29:1462–1469.

23. Solit DB, Santos E, Pratilas CA, et al. 3′-deoxy-3′-[18F]fluorothymidine positron emission tomography is a sensitive method for imaging the response of BRAF-dependent tumors to MEK inhibition. *Cancer Res.* 2007;67:11463–11469.

24. Buck AK, Kratochwil C, Glatting G, et al. Early assessment of therapy response in malignant lymphoma with the thymidine analogue [18F]FLT. *Eur J Nucl Med Mol Imaging.* 2007;34:1775–1782.

25. Apisarnthanarax S, Alauddin MM, Mourtada F, et al. Early detection of chemoradioresponse in esophageal carcinoma by 3′-deoxy-3′-3H-fluorothymidine using preclinical tumor models. *Clin Cancer Res.* 2006;12:4590–4597.

26. Yang YJ, Ryu JS, Kim SY, et al. Use of 3′-deoxy-3′-[18F]fluorothymidine PET to monitor early responses to radiation therapy in murine SCCVII tumors. *Eur J Nucl Med Mol Imaging.* 2006;33:412–419.

27. Herrmann K, Wieder HA, Buck AK, et al. Early response assessment using 3′-deoxy-3′-[18F]fluorothymidine-positron emission tomography in high-grade non-Hodgkin's lymphoma. *Clin Cancer Res.* 2007;13:3552–3558.

28. Spaepen K, Stroobants S, Dupont P, et al. [18F]FDG PET monitoring of tumor response to chemotherapy: does [18F]FDG uptake correlate with the viable tumor cell fraction? *Eur J Nucl Med Mol Imaging.* 2003;30:682–688.